

1 **Revising Contemporary Heat Flux Estimates for the Lena River, Northern Eurasia**

2 Tananaev N.I.^{1*}, Georgiadi A.G.², Fofonova V.V.³

3 ¹ Melnikov Permafrost Institute SB RAS, Yakutsk, Russia

4 ² Institute of Geography RAS, Moscow, Russia; georgiadi@igras.ru

5 ³ Alfred Wegener Institute, Helmholtz Centre for Polar and Marine Research, D-25992,
6 List, Germany; vera.fofonova@awi.de

7 * Corresponding author; TananaevNI@mpi.ysn.ru; 36 Merzlotnaya Str., Yakutsk, Sakha
8 (Yakutia) Republic, Russia, 677010

9 **Abstract**

10 The Lena River heat flux affects the Laptev Sea hydrology. Published long-term
11 estimates range from 14.0 to 15.7 EJ·a⁻¹, based on data from Kyusyur, at the river outlet.
12 A novel daily stream temperature (T_w) dataset was used to evaluate contemporary Lena
13 R. heat flux, which is 16.4±2.7 EJ·a⁻¹ (2002-2011), confirming upward trends in both T_w
14 and water runoff. Our field data from Kyusyur, however, reveal a significant negative
15 bias, -0.8°C in our observations, in observed T_w values from Kyusyur compared to cross-
16 section average T_w . Minor Lena R. tributaries discharge colder water during July-
17 September which forms a cold jet affecting Kyusyur T_w data. We show that major T_w
18 negative peaks mostly coincide with flood peaks on the Yeremeyka R., one of these
19 tributaries. This negative bias was accounted for in our reassessment. Revised
20 contemporary Lena R. heat flux is 17.6±2.8 EJ·a⁻¹ (2002-2011), and is constrained from
21 above at 26.9 EJ·a⁻¹ using data from Zhigansk, ca 500 km upstream Kyusyur. Heat flux is
22 controlled by stream temperature in June, during freshet period, while from late July to
23 mid-September, water runoff is a dominant factor.

24 **Keywords:** permafrost hydrology; Russian Arctic; the Lena river; stream temperature;
25 heat flux

26 **Introduction**

27 The terrestrial and marine compartments of the global system are connected via material
28 and energy fluxes (Huntley *et al.* 2009). In this view, rivers act as major links between
29 continents and oceans, discharging water and delivering associated fluxes to the coastal
30 zone. In the Arctic, the largest rivers bear an important thermal imprint on the adjacent
31 Arctic Ocean regions (Francis *et al.* 2009). Flowing from south to north, they are
32 immense heat conveyor belts affecting sea water temperature, ice conditions and general
33 water circulation in the Arctic and North Atlantic (Nummelin *et al.* 2016). Terrestrial
34 runoff to the Laptev Sea during summer months allows important heat accumulation in
35 the pycnocline, that affects the thermal state of submarine permafrost (Golubeva *et al.*
36 2015) and retards ice formation in autumn by 5-6 days (Kirillov 2006). Significant sea ice
37 production in the Laptev Sea compared to total Arctic Ocean ice budget and a direct link

38 between warm freshwater input and ice formation (Dmitrenko *et al.* 2009; Gutjahr *et al.*
39 2016) both add importance to the correct heat flux estimates.

40 Heat flux is a product of water discharge Q and stream temperature T_w hence it can be
41 affected by changes in both hydrologic and thermal regime under contemporary climate
42 change (van Vliet *et al.* 2013; Park *et al.* 2017). Recently, numerous studies have been
43 focusing on hydrologic change in large Arctic catchments (St. Jacques & Sauchyn 2009;
44 Yang *et al.* 2015; Tananaev *et al.* 2016; Georgiadi *et al.* 2017) and riverine heat flux
45 assessment in its potential relation to global change (Yang *et al.* 2005, 2014; Lammers *et al.*
46 *et al.* 2007; Lui & Yang 2011; Fofonova *et al.* 2017; Magritsky *et al.* 2017).

47 Published mean annual heat flux estimates of the Lena R. vary from 14.03 EJ·a⁻¹ (1950-
48 1990; Liu & Yang 2011) to 15.2 to 15.7 EJ·a⁻¹ (1935-2012; Lammers *et al.* 2007;
49 Georgiadi *et al.* 2017; Magritsky *et al.* 2017). The accuracy of these estimates relies on
50 the availability of data from long-term observation network and the quality of these data.
51 Daily T_w data are mostly unavailable for Russian rivers; hence all estimates were based
52 on 10-day averaged values, that could introduce averaging bias. Moreover, multiple
53 concerns were expressed since 1930s that T_w data from Kyusyur GS are negatively biased
54 because of cold water jet occurring along the right bank in the gauge cross-section
55 (Reinberg 1938). Modeling-based analysis performed by Fofonova *et al.* (2017) supports
56 these concerns and casts doubts on the representativeness of the stream temperature data
57 collected at Kyusyur GS. Their modeling exercises suggest observed T_w at Kyusyur being
58 *ca.* 0.8°C lower than midstream temperature or cross-section average, but these model
59 outputs, as well as previous discussions on the matter, lack direct field-based proof.
60 Based on these conclusions, Magritsky *et al.* (2017) tweak their heat flux estimate from
61 15.59 to 16.59 EJ·a⁻¹ to account for potential bias in the Kyusyur GS T_w data, but this
62 1 EJ·a⁻¹ increase lacks any justification in their paper.

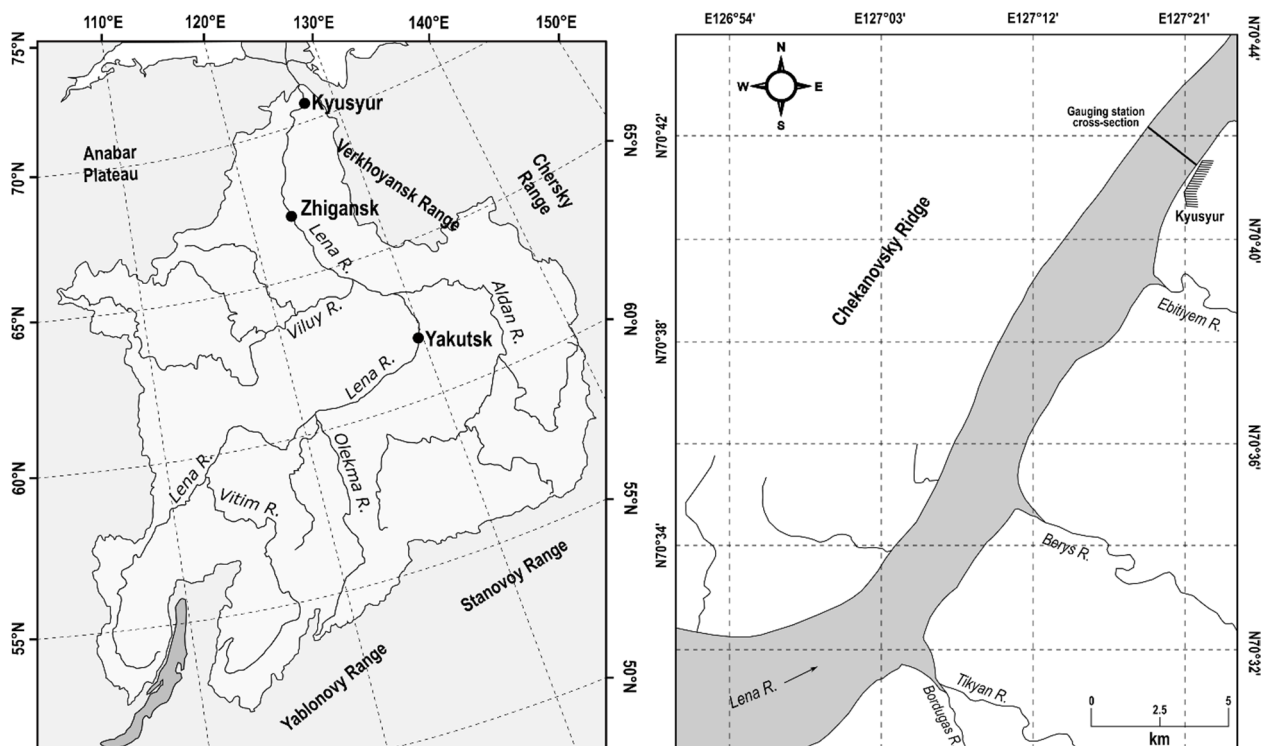
63 This paper employs a daily T_w dataset at Kyusyur GS (2002-2011; Fofonova *et al.* 2017)
64 to evaluate mean annual heat flux from daily and 10-day average data and to compare
65 these values in search for potential averaging bias. Data from our 2018 field campaign
66 are used to observe the stream temperature distribution in the Kyusyur GS cross-section,
67 to ‘ground-truth’ the existence of a cold near-bank jet and its effect on T_w values
68 measured at the gauge cross-section. Contemporary heat flux of the Lena R. is then
69 reevaluated based on daily T_w and several thermal regime scenarios, and is constrained
70 from top with heat flux estimate at Zhigansk GS, *ca.* 500 km upstream Kyusyur.

71 **Study site**

72 The Lena River, with basin area at the outlet *ca.* $2.43 \cdot 10^6$ km², drains vast areas of
73 Eastern Siberia from Lake Baikal and Transbaikalia to Anabar Plateau and west slopes of
74 the Verkhoyansk Range, and enters the Laptev Sea forming the largest delta in the Arctic
75 (Fig. 1, left). Its mean annual runoff at the outlet equals 575 km³ (2002-2011), and is

76 increasing in recent decades (e.g., Tananaev *et al.*, 2016). The catchment is almost
 77 entirely underlain by permafrost, either continuous or discontinuous (Zhang *et al.*, 1999).

78



79

80 **Fig. 1** The Lena R. basin (left) and Kyusyur GS location within the Lena R. valley (right)

81 Long-term hydrological monitoring at the Lena R. outlet is performed at Kyusyur, at a
 82 gauging station operated by Russian Hydrometeorological Agency (Roshydromet) since
 83 1935 to present (Fig. 1, right). The Lena R. flows here in a single channel about 2.5 km
 84 wide. The left bank is high and rocky, a minor spur of the Chekanovsky Ridge with
 85 elevation from 200 to 300 m a.s.l., dissected by numerous water tracks and several minor
 86 river valleys. The right bank is an alluvial terrace rising gently toward a nearby mountain
 87 chain, the Kharaulakh Ridge, where elevations range from 500 to 800 m. Numerous
 88 minor tributaries flow into the Lena R. from the right (Fig. 1, right), all draining the
 89 westward slope of the Kharaulakh Ridge.

90 The Kyusyur gauging station is located within the settlement limits, on the right bank of
 91 the Lena R., and is equipped with a pile water stage gauge. The gauging station is
 92 presently active, but open-access publication of the station data had ceased in 2012.

93 **Materials and methods**

94 This study is based on a daily stream temperature T_w dataset at Kyusyur GS, spanning
 95 from 2002 to 2011 and presented by Fofonova *et al.* (2017). This dataset originates from
 96 Tiksi Branch of Yakutian Hydrometeorological Centre, regional division of Russian
 97 Hydrometeorological Agency (Roshydromet). These data are used to: (a) calculate annual

98 heat fluxes based on daily T_w and water discharge data; (b) compare these results with
99 estimates based on 10-day T_w averages; (c) revise contemporary heat flux estimates.

100 On the Roshydromet network, T_w is measured twice daily at 8am and 8pm, near the bank,
101 using a standard mercury thermometer with a cup-protected bulb to eliminate thermal
102 inertia on reading. The thermometer is left submerged for at least 5min, then a reading is
103 taken with 0.1°C accuracy upon thermometer retrieval. Stream temperature is measured
104 daily but is only published as 10-day averaged values, and raw observed data are virtually
105 inaccessible for the scientific community. Therefore, most heat flux estimates for Russian
106 rivers are products of mean 10-day T_w and water discharge values (e.g. Lammers *et al.*,
107 2007; Magritsky *et al.*, 2017).

108 The ArcticGRO T_w data, collected in Zhigansk, *ca.* 500 km upstream Kyusyur (Holmes *et*
109 *al.*, 2018), are used in the analysis. These data are obtained using the same technique as
110 described above, but are collected bi-monthly and refer to the temperature at the moment
111 of observations, and not a daily average. Monthly averages were calculated from
112 observed values, and heat flux was estimated based on these averages.

113 Daily water discharge Q data are essential for the heat flux calculations. This study uses
114 daily Q values at two gauging stations, Lena R. at Kyusyur and Yeremeyka R. at
115 Kyusyur, provided by Tiksi Branch of Yakutian Hydrometeorological Centre. Daily Q
116 values, reported by Roshydromet offices, are not observed directly, but recalculated from
117 long-term ‘stage-discharge’ curves. Water stage is observed twice daily at 8am and 8pm
118 at pile water stage gauges at both gauging stations in question. A graduated steel rod is
119 used to obtain water level reading relative to a closest submerged pile top, which is
120 translated to water stage (above local datum) and used in water discharge calculation.
121 The accuracy of long-term stage-discharge curves is estimated to be within 5%.

122 Riverine heat flux HF , J, is calculated as:

$$123 \quad HF = C_p \cdot \rho \cdot Q \cdot T_w \cdot n \cdot t, \quad (1)$$

124 where C_p is specific heat of water, generally variable with temperature but kept constant
125 at 4186 J·kg⁻¹·K⁻¹ throughout this study; ρ is water density, 1000 kg·m⁻³, Q is water
126 discharge, m³·s⁻¹; T_w is stream temperature, °C; n is number of days in the calculation
127 interval; $t = 86400$ seconds in a day. Statistical calculations were done in RStudio (2019),
128 an integrated development environment for R language, using function *groupwiseMean()*,
129 package ‘rcompanion’ (Mangiafico, 2019).

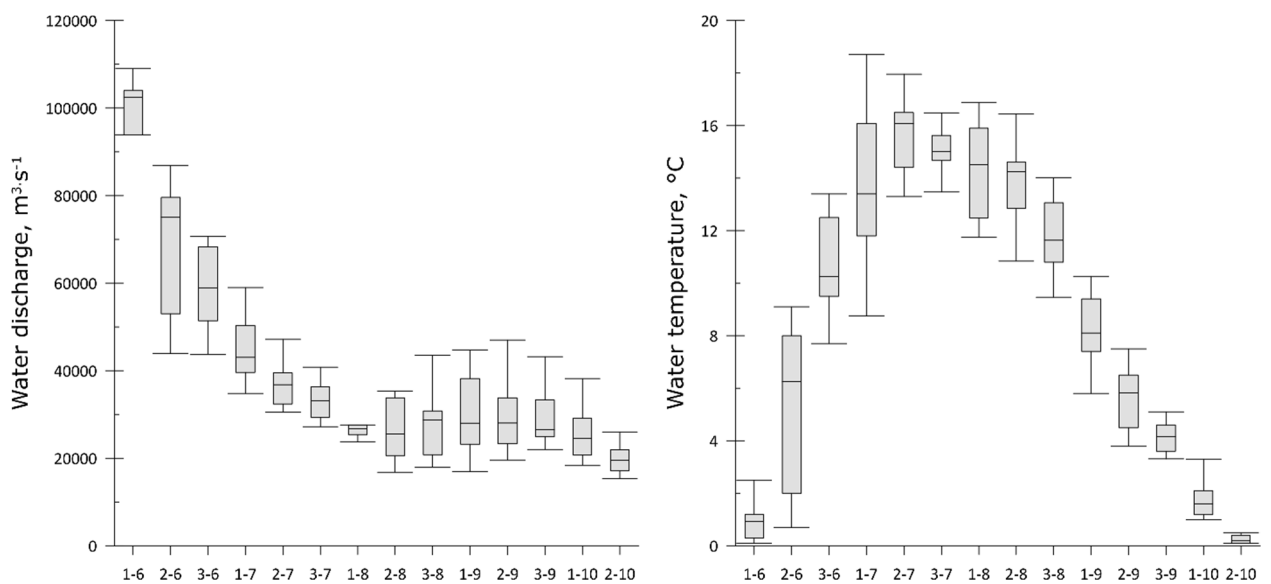
130 Field data on water temperature distribution were collected in Kyusyur in mid-August
131 2018 on the falling limb of a major rain-induced flood event originating from the
132 southern part of the Lena River basin. In the field, water temperature was measured from
133 a boat with an EXO-2 multiparameter sonde equipped with an internal temperature
134 sensor, accurate to 0.1°C with 0.01°C resolution, and a pressure/depth sensor. The sonde
135 was used to observe water temperature at various depths along seven transects at the

136 gauging station cross-section, and one longitudinal transect extending from the
 137 Ebitiyem R. mouth to the Lena R. right bank (Fig. 1, right).

138 **Results**

139 *The Lena River T_w and heat flux, 2002-2011*

140 The open-water period at the Lena R. outlet starts around early June. The stream
 141 temperature rises above 0.2°C several days before the ice breakup, on 2 June (average,
 142 2002-2011). At this moment, water discharge peaks, exceeding 100 000 m³·s⁻¹ (Fig. 2,
 143 left). Both Q and T_w vary greatly at the falling limb of the freshet, affecting the variability
 144 in resulting heat fluxes. The freshet signal fades away by mid-July. Low-flow period ends
 145 by mid-August, then water discharge oscillates until freeze-up because of numerous rain
 146 floods originating from the Lena R. headwaters.



147

148 **Fig. 2** Water discharge and stream temperature of the Lena R. at Kyusyur by 10-day periods. On
 149 x -axis, 10-day period numbers and months, separated by a hyphen. Boxplots mark median, 25%
 150 and 75% quartiles, and whiskers match interquartile range x 1.5

151 Stream temperature reaches its maximum values, between 14°C and 16°C on average, by
 152 early to mid-July, then remains at this plateau until mid-August, and gradually decreases
 153 to 0.2°C by mid-October (Fig. 2, right). Mean highest daily T_w is $18.5 \pm 1.5^\circ\text{C}$ and is
 154 observed in July. Multiple publications claim upward trends in T_w in recent decades
 155 (Yang *et al* 2005; Liu & Yang 2011; Georgiadi *et al* 2017; Magritsky *et al* 2017); our
 156 results support these conclusions.

157 In numerous preceding publications, heat flux of the Lena R. at Kyusyur GS is assessed
 158 using published 10-day averages (1935-2012; Georgiadi *et al.* 2017; Lammers *et al.*
 159 2007; Magritsky *et al.* 2017). Here, the daily T_w dataset is used in calculations along with
 160 10-day averages; Eq. 1 was used in calculations. Data analysis reveals no averaging bias
 161 related to the use of 10-day average T_w is lieu of daily values; the two estimates being

162 identical at $16.4 \pm 2.7 \text{ EJ} \cdot \text{a}^{-1}$. This is substantially higher than previous estimates, and is
163 close to $16.04 \text{ EJ} \cdot \text{a}^{-1}$ estimate for 1980-2012, published by Magritsky (2016).

164 *The Lena R. water temperature distribution*

165 Besides averaging bias, the T_w data from Kyusyur GS are reported to be negatively
166 biased, affected by a cold jet in the near-bank zone (Reinberg 1938). Our field data from
167 the 2018 campaign confirm this report.

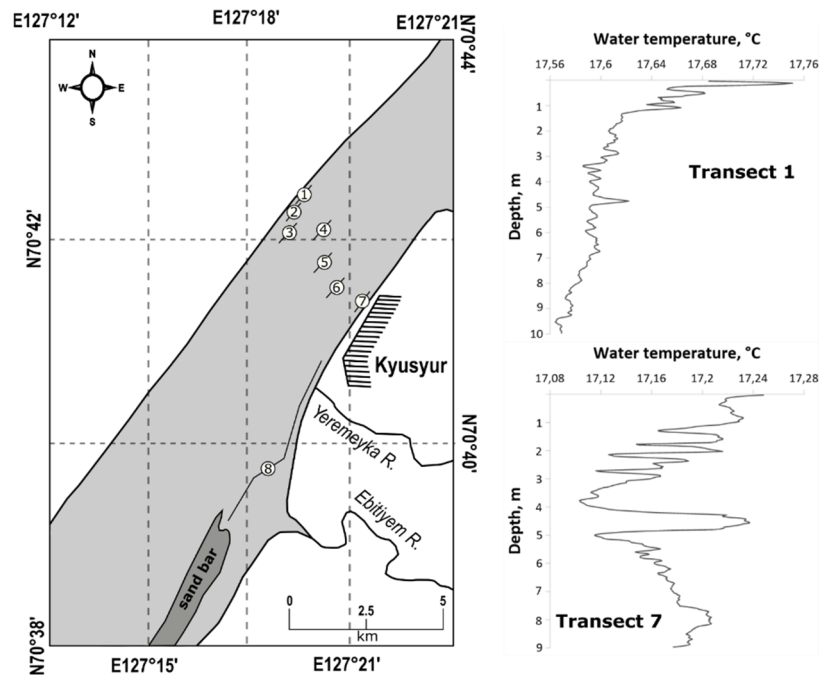
168 Water temperature distribution at the Kyusyur GS cross-section is found to be mostly
169 uniform in both vertical (surface to bottom) and lateral (bank to bank) directions. Vertical
170 temperature distribution is uniform at least in the first 7 to 10 m of the water column,
171 evidencing strong turbulent mixing in the cross-section, reserve observation points
172 adjacent to riverbanks (Table 1, Fig. 3). At Transect 1, near the left bank, water
173 temperature decreases with depth by only 0.18°C within 10 m, while at Transect 7, along
174 the right bank, several distinct water masses are observed, the one at 4 m depth having
175 properties resembling those of the surface waters (Fig. 3, right).

176 **Table 1**
177 Water temperature of the Lena R. at transects in the Kyusyur GS cross-section (see Fig. 3 for
178 spatial reference; observations made 15 August 2018)

Transect	Depth d , m	Surface T_w , $^\circ\text{C}$	T_w at depth d , $^\circ\text{C}$	Mean T_w , $^\circ\text{C}$
1	10	17.75	17.57	17.6
2	7	17.76	17.76	17.76
3	7	17.84	17.82	17.83
4	7	17.9	17.9	17.9
5	8	18.0	17.98	18.0
6	9	17.9	17.88	17.9
7	9	17.2	17.1	17.15

180

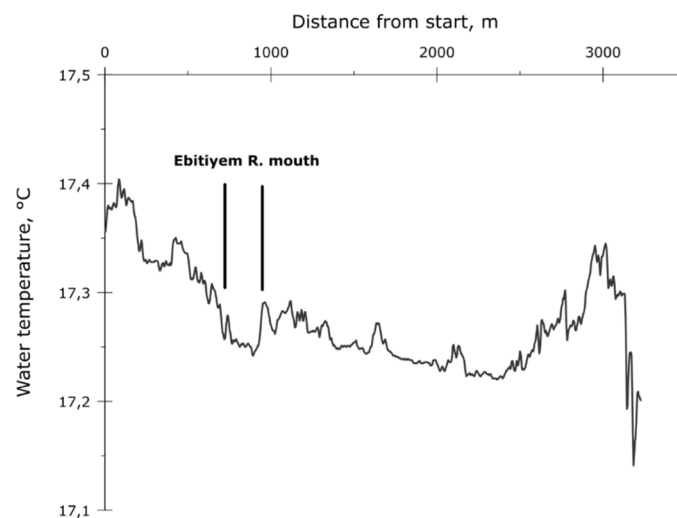
181 In lateral direction, lower temperature values were observed near the banks of the
182 Lena R. Midstream water temperature was around 17.9 to 18.0°C , but it was by 0.4°C
183 lower at Transect 1, and by 0.85°C at Transect 7 (Table 1). Thermal impact of minor
184 tributaries, heat exchange with channel bottom, cooling influence of permafrost or stream
185 circulation patterns may be deemed responsible for these anomalies.



186

187 **Fig. 3** Water temperature observation points near Kyusyur GS (left), vertical temperature
 188 profiles at near-bank transects (right)

189 The minor mountainous right-hand tributaries were suggested to produce this relatively
 190 cold jet along the right bank of the Lena River (Fofonova *et al.*, 2017). A transect was
 191 then planned to track longitudinal gradient in water temperature around the mouth zone
 192 of such tributaries. The closest tributary upstream from Kyusyur is the Yeremeyka R.
 193 (Fig. 3, left), but it had completely dried out at the time of our fieldwork. Observations
 194 were then performed at the mouth of a larger river, the Ebitiyem R., from a moving boat
 195 with a sensor submerged at *ca.* 0.5 m depth. Data from this longitudinal transect between
 196 the Ebitiyem R. mouth to the Lena R. right bank, confirm that thermal imprint of this
 197 tributary is significant and persists at least as far as the gauging station area (Fig. 4).



198

199 **Fig. 4** The Lena R. surface water temperature along the Transect 8, see Fig. 3, right, for
 200 reference

201 Upstream the tributary mouth, water was already cooler than at midstream, ca. 17.4°C,
202 and a further decrease down to 17.2°C is corresponding to the tributary inflow. This
203 pattern continues toward the gauging station, where water temperature drops further to
204 17.1°C (Fig. 4). A 1.5°C decrease in water temperature toward the end of the transect
205 was observed where the survey boat approached the right bank and was about 100 m
206 from the shoreline.

207 Field results prove the incoherence of the T_w data reported by Kyusyur GS, with the
208 temperature difference between midstream and near-bank, ΔT_w , reaching 0.85°C.
209 Discharge-weighted cross-sectional average T_w is not expected to be significantly lower
210 than midstream, since ‘colder’ channel sections adjacent to riverbanks are relatively
211 shallow and have lower velocity. Detailed seasonal surveys are to be performed to relate
212 observations at Kyusyur GS to cross-section average T_w .

213 *Scenario-based Lena R. heat flux reassessment*

214 The Lena R. heat flux for the 2002-2011 period was reassessed upon collecting field
215 evidences that the T_w values observed at Kyusyur GS are misrepresentative for the cross-
216 section average. A correction factor ΔT_w , either constant or time-dependent, was
217 introduced in the observed data. Its value cannot be derived from a single field survey,
218 hence modeling results presented in (Fofonova *et al.*, 2017) were used in scenario
219 building. Two simple hypothetical scenarios were developed, for constant or time-
220 dependent ΔT_w . For all scenarios, $\Delta T_w = 0^\circ\text{C}$ for May, June and October.

221 Scenario 1: $\Delta T_w = +0.8^\circ\text{C}$ for July, August and September. This ΔT_w value is a simulated
222 mean difference between cross-section average T_w and near-bank T_w observed at Kyusyur
223 GS (Fofonova *et al.*, 2017, Fig. 9a), and is surprisingly close to our field results. This
224 correction increases the Lena R. heat flux to $17.3 \pm 2.8 \text{ EJ}\cdot\text{a}^{-1}$ (2002-2011) *i.e.* by 5%
225 compared to uncorrected value.

226 Scenario 2: is based on the previous scenario, but accounts for extreme temperature
227 gradients that could be observed throughout the open-water period. Simulated daily ΔT_w
228 values were up to $+3.0^\circ\text{C}$ in July 2011 and August 2007, and up to $+5^\circ\text{C}$ in September
229 2003 on certain days (Fofonova *et al.* 2017). Highest monthly average ΔT_w values were
230 $+2.0^\circ\text{C}$ in July and August, and $+3.0^\circ\text{C}$ in September.

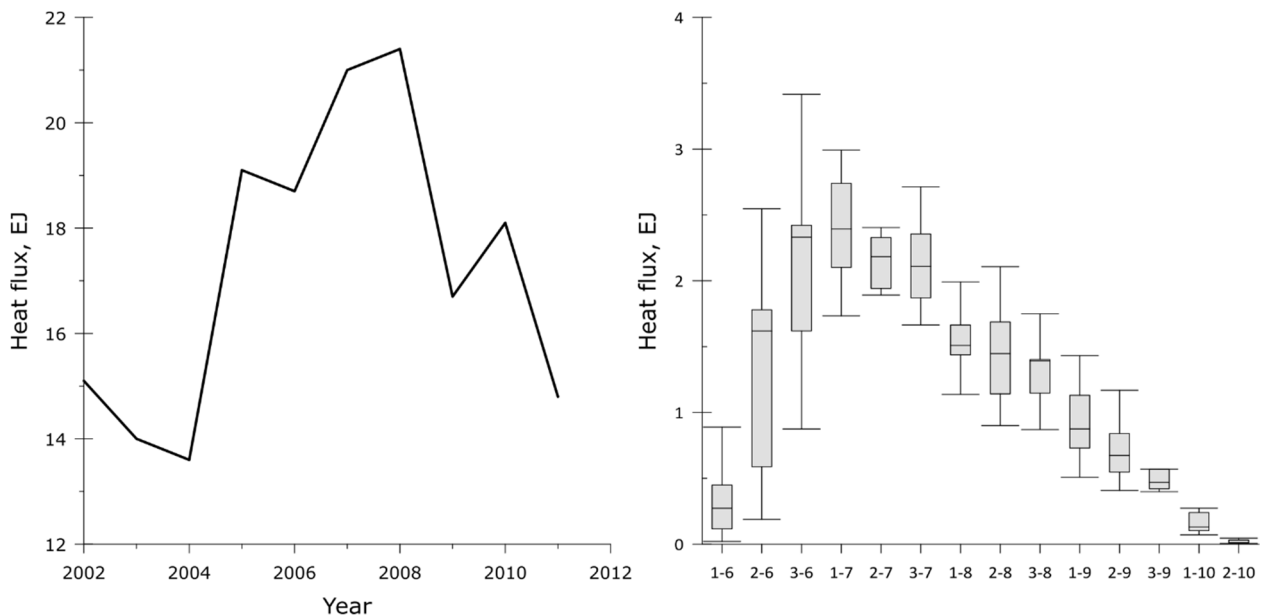
231 Monthly ΔT_w variation scenarios were formulated as follows, allowing temperature
232 anomalies in one of three months (Cases 2-4), two (Cases 5-7) or in all three months
233 (Case 8):

- 234 (1) July-September, $\Delta T_w = +0.8^\circ\text{C}$, same as Scenario 1;
235 (2) July, $\Delta T_w = +2.0^\circ\text{C}$; August-September, $\Delta T_w = +0.8^\circ\text{C}$;
236 (3) July & September, $\Delta T_w = +0.8^\circ\text{C}$; August, $\Delta T_w = +2.0^\circ\text{C}$;
237 (4) July & August, $\Delta T_w = +0.8^\circ\text{C}$; September, $\Delta T_w = +3.0^\circ\text{C}$;
238 (5) July & August, $\Delta T_w = +2.0^\circ\text{C}$; September, $\Delta T_w = +0.8^\circ\text{C}$;

- 239 (6) July, $\Delta T_w = +2.0^\circ\text{C}$; August, $\Delta T_w = +0.8^\circ\text{C}$; September, $\Delta T_w = +3.0^\circ\text{C}$;
240 (7) July, $\Delta T_w = +0.8^\circ\text{C}$; August, $\Delta T_w = +2.0^\circ\text{C}$; September, $\Delta T_w = +3.0^\circ\text{C}$;
241 (8) July & August, $\Delta T_w = +2.0^\circ\text{C}$; September, $\Delta T_w = +3.0^\circ\text{C}$.

242 These distributions have differing frequencies of occurrence, or return periods, which are
243 unknown for general population, so sample frequencies were used in further analysis.
244 Cases 2-4 each occur once in 10 years, then Cases 5-7 – once in 100 years, and Case 8
245 once in 1000 years. Case 1 takes what is left, or 889 years out of 1000. Heat fluxes were
246 calculated for each year of record and for each case, then this dataset was bootstrapped
247 with number of permutations $n = 10000$ accounting for frequencies of occurrence.
248 Revised contemporary mean annual Lena R. heat flux is estimated at $17.6 \pm 2.8 \text{ EJ}\cdot\text{a}^{-1}$
249 (2002-2011; Fig. 5), corrected for ΔT_w extremes and accounting for their return periods.

250



251

252 **Fig. 5** Revised annual Lena R. heat flux, 2002-2011, and its distribution across 10-day periods.
253 On x -axis, 10-day period numbers and months, separated by a hyphen. Boxplot marks median,
254 25% and 75% quartiles, and whiskers match interquartile range $\times 1.5$

255 The Lena R. heat flux appears to vary highly across years (Fig. 5). At a monthly scale,
256 late June fluxes are highly variable and could mark annual maximum; on average,
257 however, the latter is observed in July, when the freshet is still at its falling limb and
258 highest T_w are observed.

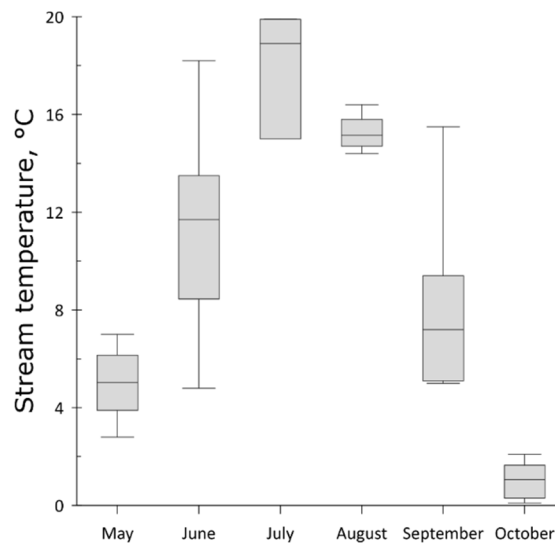
259 Discussion

260 *Constraining Lena R. heat flux estimate*

261 The revised estimate is based on modeling results, assuming a virtually constant ΔT_w
262 value. Its lower bound constraint can be easily estimated at $16.4 \text{ EJ}\cdot\text{a}^{-1}$, *i.e.* estimated heat
263 flux before temperature corrections. The upper bound constraint is hard to assess based

264 on data from Kyusyur GS, since the true ΔT_w and its temporal variation are unknown.
265 The ArcticGRO T_w dataset collected in Zhigansk GS, about 500 km upstream from
266 Kyusyur, is used to evaluate the upper bound constraint. Water discharge data from
267 Kyusyur GS are used in calculations, since the gauging station in Zhigansk had never
268 observed this parameter.

269 In total, ArcticGRO database contains 38 T_w observations from 2003 to 2018, covering
270 the open water period from mid-May to early October. These observations were averaged
271 across months (Fig. 6). These are rough estimates since T_w measurements are unevenly
272 distributed throughout months, but they are based on the only data which are openly
273 available. Corresponding mean monthly water discharge values at Kyusyur GS for 2002-
274 2011 period were used in calculations.



275

276 **Fig. 6** Mean monthly stream temperature, the Lena R. at Zhigansk GS, ArcticGRO data (Holmes
277 *et al.* 2018)

278 Mean annual heat flux at Zhigansk GS equals $26.9 \text{ EJ}\cdot\text{a}^{-1}$ (2003 to 2011) and can serve as
279 an extreme upper bound to constrain the heat flux observed at Kyusyur GS, supposing
280 that total heat turnover in the stream is maintained at zero level as water travels from
281 Zhigansk to Kyusyur.

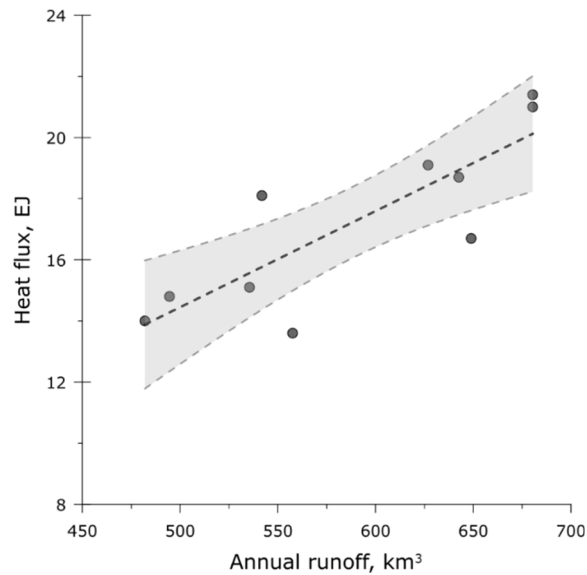
282 *Hydrological controls over the Lena R. heat flux*

283 Riverine heat flux is controlled by water discharge and stream temperature, both highly
284 variable. In a long-term perspective, heat flux of the Lena R. is mostly controlled by
285 water runoff (Fig. 7). The following linear equation describes this relation ($r = 0.84$,
286 $p < 0.01$):

$$287 \quad HF = 0.0315 \cdot W_Q - 1.28, \quad (2)$$

288 where HF – annual heat flux, EJ; W_Q – annual runoff, km^3 .

289



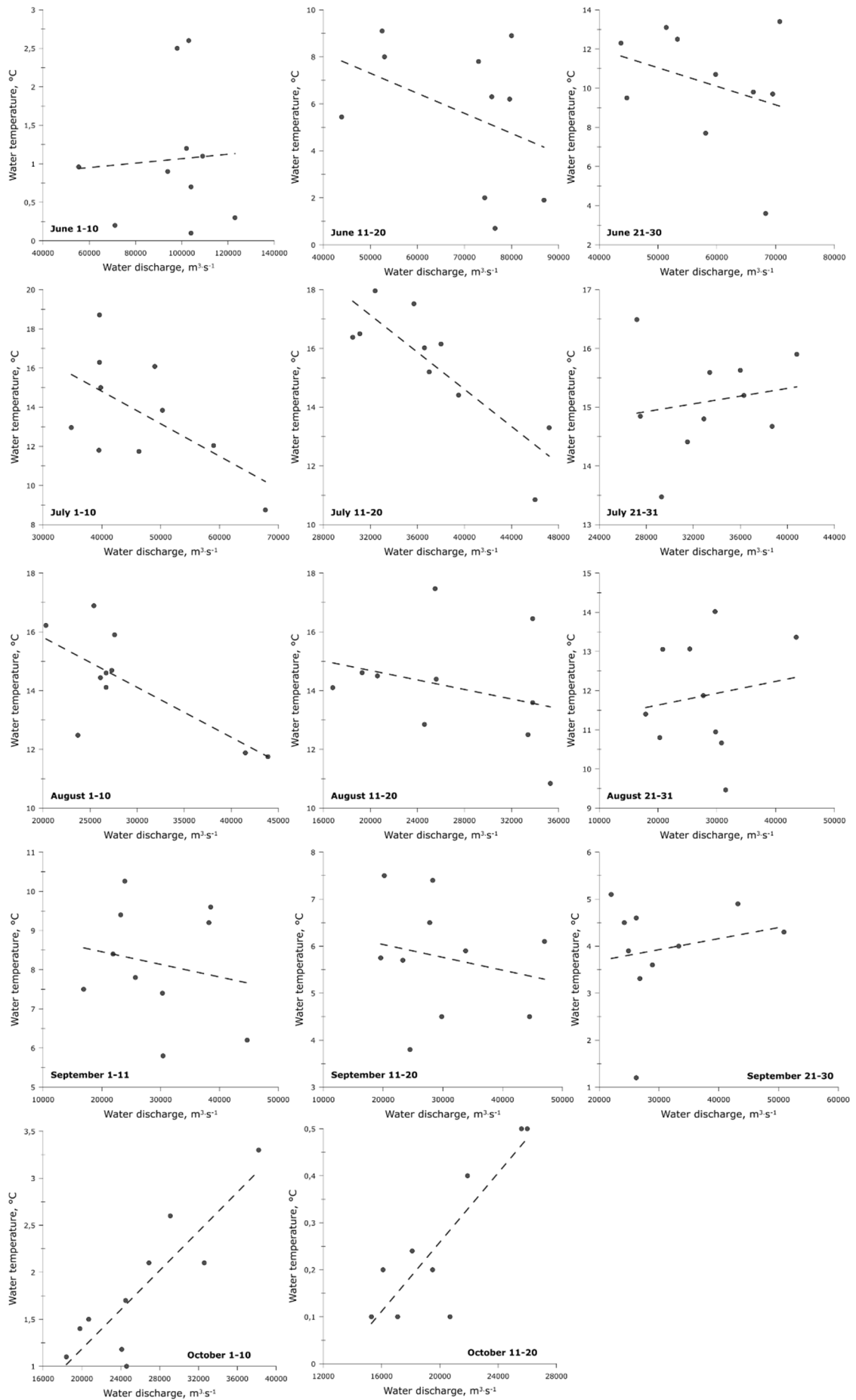
290

291 **Fig. 7** The Lena R. annual heat flux related to annual runoff at Kyusyur GS, 2002-2011

292 However, at sub-annual scale, water discharge and stream temperature seem to mostly act
 293 as two independent controls over heat flux. For most of the year, these two parameters
 294 are mutually independent at a 10-day scale, with a slight tendency toward lower T_w
 295 values at higher discharges (Fig. 8). Notable exceptions include early and mid-July, when
 296 T_w is decreasing with higher Q , and October, when this same relation is positive.

297 Falling limb of a freshet generally continues to mid-July, and high discharge at this time
 298 corresponds to the overlapping rain events. The latter originate from the mountainous
 299 southern part of the basin, where permafrost groundwater and numerous icings may
 300 influence stream temperature. However, their thermal impact is expected to be negligible,
 301 as this water should accumulate heat during its 2000 km descent to Kyusyur. Hence
 302 closer sources are to be thought of. The Vilyui R. is regulated by a large hydropower
 303 station, discharging colder waters, but its water temperature returns to equilibrium values
 304 by the river mouth (Magritsky, 2016). The retarded freshet or juxtaposed rain floods on
 305 the Aldan River (Fig. 1, left) could be responsible for this temperature decline. Most of
 306 its basin is mountainous, where icings are abundantly present, and flash floods are
 307 common on its right tributaries upstream the Lena-Aldan confluence.

308 In October, higher runoff is also related to rain events, but at this time, the most distant
 309 sources of warmer water are at play. Longer travel time assures higher heat accumulation
 310 may be partly related to heat release from the alluvial channel and floodplain. The Lena
 311 R. channel between Yakutsk and Zhigansk accommodates enormous sand bars, that are
 312 drained and exposed to sunlight at low levels. Their prolonged inundation toward the end
 313 of autumn might serve an important heat source, as previously suggested by Fofonova *et*
 314 *al* (2017), yet never assessed directly.



315

316

Fig. 8 The Lena R. water discharge related to 10-day average T_w , Kyusyur GS (2002-2011)

317 When water discharge and temperature are correlated, both are controlling heat flux.
 318 When no relation is observed, both fluctuate chaotically and none has a unique control on
 319 heat flux. However, two distinct periods with both Q -controlled and T_w -controlled heat
 320 flux emerge in our analysis. Temperature-controlled heat flux is observed throughout
 321 June, while most of the open-water period the Lena R. heat flux is discharge-controlled
 322 (Table 2).

323 **Table 2**
 324 Discharge- vs water temperature-controlled heat flux periods, the Lena R. at Kyusyur
 325

Period	R^2, Q vs HF	R^2, T_w vs HF	Pattern
June 1-10	0.04	0.98	T_w -controlled
June 11-20	$3 \cdot 10^{-5}$	0.83	T_w -controlled
June 21-30	0.07	0.68	T_w -controlled
July 1-10	0.15	0.24	
July 11-20	0.12	0.04	
July 21-31	0.91	0.22	Q -controlled
August 1-10	0.80	0.12	Q -controlled
August 11-20	0.69	0.08	Q -controlled
August 21-31	0.85	0.27	Q -controlled
September 1-10	0.66	0.16	Q -controlled
September 11-20	0.72	0.11	Q -controlled
September 21-30	0.77	0.41	
October 1-10	0.86	0.96	
October 11-20	0.87	0.96	

326 Values in **bold** are significant at $p < 0.01$

327 This apparent seasonality stems from this large river hydrology. During the freshet, water
 328 discharge is enormously high, occasionally exceeding $150\,000\text{ m}^3 \cdot \text{s}^{-1}$, and even slightly
 329 warmer water will produce disproportionately high HF response compared to other
 330 periods. From the end of July to late September, the variation in T_w decreases since the
 331 major heat source across the basin is solar radiation (see Fig. 2, right), and the amount of
 332 water takes over the total heat flux value for these periods.

333 This pattern has long-standing implications from the climate change perspective. We can
 334 assume that climate change effects on the Lena R. heat flux would be less significant if
 335 they will be related to: (a) water discharge increase in June, *e.g.* higher snow water
 336 equivalent during winter or higher rainfall around the freshet peak; (b) water temperature
 337 increase in August-September, *e.g.* persistent high pressure over central Yakutia or less
 338 impact from cooler mountainous rivers. In contrast, (c) an increase in June water
 339 temperature, associated with earlier onset of summer, or (d) rainfall runoff increase
 340 throughout July and August, caused by heavy rains in the Vitim and Olyokma R. basins,
 341 will lead to pronounced heat flux increase in Kyusyur and in the Lena Delta region. In all
 342 cases, runoff/temperature increase in October will lead to higher heat flux.

343 *Cold water origin in the Lena R. channel*

344 Cold water jet along the right bank of the Lena R. originates from minor right-bank
 345 tributaries, as suggested by modeling results (Fofonova *et al.* 2017) and confirmed by our
 346 field observations. While flow may cease during summer on smaller creeks, like the
 347 Yeremeyka R. with basin area of 9.7 km², the larger tributaries maintain their flow
 348 throughout the rain-free period. The thermal impact of these minor tributaries, already
 349 significant under low-flow conditions, may increase drastically during heavy rains in
 350 their basins. This effect was traced in the T_w data observed at Kyusyur GS, using daily
 351 discharge data from the Yeremeyka R. at Kyusyur, a gauging station at the outlet of a
 352 minor Lena R. tributary (see Fig. 3, left). In most cases, the T_w in Kyusyur drops
 353 significantly at the time of the flood peak at the Yeremeyka R., which in this analysis
 354 represents all minor right tributaries (Table 3). This effect is present at various Lena R.
 355 discharges, up to 78100 m³·s⁻¹. It is less pronounced in September, and can exceed 2.5°C
 356 in July (Table 3). These data strongly support the origin of the cold near-bank water from
 357 minor right-hand tributaries of the Lena R.

358

359

360

Table 3

Thermal effect of the rain flood peaks on the right-bank tributaries, represented by the
 Yeremeyka R., on the Lena R. T_w at Kyusyur GS, 2002-2011

Year	Flood peak, Yeremeyka R.		Minimum T_w at Kyusyur			
	Date	Q , m ³ ·s ⁻¹	Date	Q , m ³ ·s ⁻¹	Min T_w , °C	Off-min T_w , °C*
2002	29.07	2.34	31.07	35400	10.9	11.7
2003	29.07	1.26	30.07	32200	10.9	14.3
	08.09	3.14	09.09	25600	3.9	5.2
2004	30.08	1.22	01.09	30100	7.8	8.0
2005	30.08	1.09	01.09	46200	6.5	7.0
	19.09	0.66	22.09	35200	3.8	3.9
2006	24.07	1.58	24.07	34200	11.5	12.3
	06.08	1.25	06.08	26100	15.5	16.3
	18.09	0.74	–	–	–	–
2007	18.06	1.29	19.06	78100	8.3	9.8
	11.07	1.58	11.07	44400	8.6	11.6
	01.08	2.71	04.08	42300	10.7	11.8
2008	28.08	0.49	–	–	–	–
2009	04.09	0.74	04.09	30800	4.5	5.1
	09.09	0.74	09.09	31200	4.8	5.6
2010	28.06	0.73	–	–	–	–
	27.07	1.51	28.07	40200	14.9	15.2
	01.09	0.45	02.09	22500	10.6	10.8
2011	09.07	0.72	09.07	30000	12.3	13.4
	17.07	1.14	–	–	–	–
	27.07	0.68	29.07	25200	14.8	15.3

361

* Calculated as average T_w of the two days adjacent to the minimum T_w date in Kyusyur GS

362 The potential sources of this cold storm- and baseflow are numerous, snow and icings
363 meltwater, and groundwater flow among the most important.

364 Snow cover in this High Arctic region normally decays by early June, but remnant snow
365 patches may persist until late July and even to mid-August in shaded valleys, on
366 mountain slopes and in the peak areas of the Kharaulakh Range. Thermal impact of
367 melting snow on water temperature during summer months is probably negligible, since
368 meltwater from these snow patches is not directly connected to streamflow.

369 Icings are common permafrost hydrology features (Pinneker, 1990; Yoshikawa *et al.*,
370 2007). Normally, medium and large icings of the Verkhoyansk region completely decay
371 by late August, and only the largest ones are capable of surviving one or more summers.
372 Their contribution to river runoff may reach significant proportions, up to 12% of total
373 basin discharge (Clark, Lauriol, 1997), particularly important during baseflow period, but
374 also during heavy rainfall, when the flood wave leads to ice deterioration and decay. Cold
375 icing water is directly connected to streams and may play a significant role in water
376 cooling. Several typical icing fields in the Tikyan R. basin are detectable using satellite
377 imagery.

378 Groundwater flow has minor influence on river runoff in the continuous permafrost
379 regions, but the presence of icings confirms groundwater discharge in the valleys of
380 minor Lena R. tributaries. Regional observations on groundwater temperature are absent,
381 but most springs are reported to have water temperatures close to 0°C under similar
382 conditions in northeastern Alaska (Kane *et al.*, 2013).

383 *Implications for other Russian Arctic gauging stations*

384 Our results show that local hydrology may interfere severely with the accuracy of routine
385 stream temperature observations. To this end, data from the major Russian Arctic river
386 outlets should be analysed for relevance. At the Yenisey R. outlet, stream temperature is
387 observed at Igarka GS. This gauging station is situated on the right bank of the Igarskaya
388 Branch, a large side channel receiving numerous tributaries upstream the GS cross-
389 section. The Ob R. outlet is at Salekhard GS, where the gauging station is situated on the
390 right bank of a secondary branch in a highly braded section. In theory, the data from
391 these stations can also be biased and misrepresent the cross-section average T_w . If this is
392 the case, then the total heat flux from the Russian Arctic rivers is undervalued, affecting
393 the quality of ocean circulation model outputs.

394 **Conclusions**

395 This study confirms, with both published and field data, that stream temperature
396 observations at Kyusyur GS are misrepresentative neither for midstream nor the cross-
397 sectional average temperatures.

398 During our field survey, the water temperature at the observation point of Kyusyur GS,
399 *ca.* 3 m from the river bank, was found to be by 0.85°C lower than midstream
400 temperature, which is surprisingly close to previous modeling results (Fofonova *et al.*,
401 2017). Field data evidence the existence of a relatively cold-water jet extending at least
402 150 m from the right Lena R. bank toward midstream.

403 We conclude therefore that existing heat flux calculations for the Lena R. at Kyusyur are
404 negatively biased. The thermal impact of minor upstream tributaries is shown to be a
405 major reason for this misrepresentation, and to increase during rain floods on these
406 tributaries.

407 Revised Lena R. heat flux estimate, corrected for this negative bias, is $17.6 \pm 2.8 \text{ EJ}\cdot\text{a}^{-1}$.
408 From the upper bound, our estimate is constrained at $26.9 \text{ EJ}\cdot\text{a}^{-1}$, obtained using monthly-
409 averaged T_w data from Zhigansk GS, *ca.* 500 km upstream Kyusyur. During most of the
410 year, water discharge is controlling heat flux value, but in June, the latter is totally
411 controlled by stream temperature.

412 **Acknowledgements**

413 This study is partially funded by Russian Fund for Basic Research, Project 17-05-00948
414 (hydrological analysis and heat flux calculations), Project 18-05-60240-ARCTIC (field
415 investigations). The authors are grateful to Afanasiy Popov (technician, Kyusyur GS,
416 Roshydromet) and other locals for the assistance in the 2018 fieldwork.

417 **Author contributions.** Conceptualization, methodology, investigation, formal analysis,
418 writing – original draft, N.T.; Funding acquisition, investigation, A.G.; Resources, V.F.;
419 Data curation, N.T. and V.F. All authors contributed to discussions, review and editing of
420 the original draft.

421 **References**

- 422 Clark I.D., Lauriol B. (1997) Aufeis of the Firth River basin, Northern Yukon, Canada: Insights
423 into permafrost hydrogeology and karst, *Arctic and Alpine Research* **29**(2), 240–252.
- 424 Dmitrenko I.A., Kirillov S.A., Tremblay L.B., Bauch D. & Willmes S. (2009) Sea-ice production
425 over the Laptev Sea shelf inferred from historical summer-to-winter hydrographic observations
426 of 1960s-1990s, *Geophys. Res. Lett.* **36**, L13605, doi: 10.1029/2009GL038775.
- 427 Fofonova V., Zhilyaev I., Kraineva M., Iakshina D., Tananaev N., Volkova N., Sander L.,
428 Papanmeier S., Michaelis R. & Wiltshire K.H. (2017) Features of the water temperature long-
429 term observations on the Lena River at basin outlet, *Polarforschung* **87**(2), 135-150.
- 430 Francis J.A., White D.M., Cassano J.J., Gutovski Jr. W.J., Hinzman L.D., Holland M.M., Steele
431 M.A. & Vörösmarty C.J. (2009) An arctic hydrologic system in transition: Feedbacks and
432 impacts on terrestrial, marine, and human life, *J. Geophys. Res.* **114**, L04019, doi:
433 10.1029/2008JG000902.

- 434 Georgiadi A.G., Kashutina E.A. & Milyukova I.P. (2017) Long-term changes of water flow,
435 water temperature and heat flux of the largest Siberian rivers, *Polarforschung* **87(2)**, 167-176.
- 436 Golubeva E., Platov G., Malakhova V., Iakshina D. & Kraineva M. (2015) Modeling the impact
437 of the Lena River on the Laptev Sea summer hydrography and submarine permafrost state, *Bull.*
438 *Nov. Comp. Center* **15**, 13-22.
- 439 Gutjahr O., Heinemann G., Preußner A., Willmes S. & Drüe C. (2016) Quantification of ice
440 production in Laptev Sea polynyas and its sensitivity to thin-ice parameterizations in a regional
441 climate model, *The Cryosphere* **10**, 2999–3019.
- 442 Holmes R.M., McClelland J.W., Tank S.E., Spencer R.G.M. & Shiklomanov A.I. (2018) Arctic
443 Great Rivers Observatory. Water Quality Dataset. Version 20181010.
444 <https://www.arcticgreatrivers.org/data>
- 445 Huntley D.A., Leeks G.J.L. & Walling D. (2009) From rivers to coastal seas: the background
446 and context of the land-ocean interaction study. In: Land-Ocean Interaction (Huntley D.A.,
447 Leeks G.J.L., Walling D., eds), IWA Publ. House, London, UK, pp. 1-8.
- 448 Kane D.L., Yoshikawa K. & McNamara J.P. (2013) Regional groundwater flow in an area
449 mapped as continuous permafrost, NE Alaska (USA), *Hydrogeology J.*, **21(1)**, 41-52.
- 450 Kirillov S.A. (2006) Spatial variation in sea-ice formation-onset in the Laptev Sea as a
451 consequence of the vertical heat fluxes caused by internal waves overturning, *Polarforschung*
452 **76(3)**, 119-123.
- 453 Lammers R.B., Pundsack J.W. & Shiklomanov A. (2007) Variability in river temperature,
454 discharge and energy flux from the Russian pan-Arctic landmass, *J. Geophys. Res.* **112**, G04S59,
455 doi: 10.1029/2006JG000370.
- 456 Liu B., Yang D. (2011) Siberian Lena River heat flow regime and change, IAHS Publ. 346, 71-
457 76.
- 458 Magritsky D.V. (2016) Factors and trends of the long-term fluctuations of water, sediment and
459 heat runoff in the lower reaches of the Lena River and the Vilyui River, *Bull. Moscow State*
460 *University, Series 5 Geography*, **No. 6**, 85–94 (in Russian).
- 461 Magritsky D., Alexeevsky N., Aybulatov D., Fofonova V. & Gorelkin A. (2017) Features and
462 evaluations of spatial and temporal changes of water runoff, sediment yield and heat flux in the
463 Lena River delta, *Polarforschung* **87(2)**, 89-110.
- 464 Mangiafico S. (2019) ‘rcompanion’: Functions to support extension education program
465 evaluation.
- 466 Nummelin A., Ilicak M., Li C. & Smedsrud S.H. (2016) Consequences of future increased Arctic
467 runoff on Arctic Ocean stratification, circulation and sea ice cover, *J. Geophys. Res.* **121(1)**, 617-
468 637.
- 469 Park H., Yoshikawa Y., Yang D. & Oshima K. (2017) Warming water in Arctic terrestrial rivers
470 under climate change, *J. Hydromet.* **18(7)**, 1983-1995.

- 471 Pinneker Ye.V. (1990) Groundwater monitoring and management in permafrost areas, IAHS
472 Publ. 173, 39-44.
- 473 Reinberg A.M. (1938): Hydrology of Soviet Arctic Rivers: Hydrology information about Lena,
474 Ebitiem, Indigirka, Hatanga, Yenisei and Kolyma Rivers. *Proceed. Arctic Antarctic Res. Institute*
475 **105**, 51-72 (in Russian).
- 476 RStudio: Integrated Development Environment for R (version 1.1.447). Computer Software,
477 Boston, VA, USA (Retrieved 1 April 2019).
- 478 St. Jacques, J. M., Sauchyn D.J. (2009), Increasing winter baseflow and mean annual streamflow
479 from possible permafrost thawing in the Northwest Territories, Canada, *Geophys. Res. Lett.*
480 **36(1)**, L01401, doi: 10.1029/2008GL035822.
- 481 van Vliet M.T.H., Franssen W.H.P., Yearsley J.R., Ludwig F., Haddeland I., Lettenmaier D.P. &
482 Kabat P. (2013) Global river discharge and water temperature under climate change, *Glob*
483 *Environ Change* **23(2)**, 450-464, doi: 10.1016/j.gloenvcha.2012.11.002.
- 484 Yang D., Liu B. & Ye B. (2005) Stream temperature changes over Lena River Basin in Siberia,
485 *Geophys Res Lett* **32(5)**, L05401, doi: 10.1029/2004GL021568.
- 486 Yang D., Marsh P. & Ge S. (2014) Heat flux calculations for Mackenzie and Yukon Rivers,
487 *Polar Science* **8(3)**, 232-241, doi: 10.1016/j.polar.2014.05.001.
- 488 Yang, D., X. Shi & Marsh P. (2015), Variability and extreme of Mackenzie River daily
489 discharge during 1973–2011, *Quat. Int.*, **380–381**, 159–168, doi: 10.1016/j.quaint.2014.09.023.
- 490 Yoshikawa K.; Hinzman L.D. & Kane D.L. (2007) Springs and aufeis (icing) hydrology in
491 Brooks Range, Alaska, *J. Geophys. Res.* **112**, G04S43, doi:10.1029/2006JG000294.
- 492 Zhang T., Barry R.G., Knowles K., Heginbottom G.A. & Brown J. (1999) Statistics and
493 characteristics of permafrost and ground-ice distribution in the Northern Hemisphere, *Polar*
494 *Geogr.* **23(2)**, 132-154.